

On electronic properties from the application of field dependence SSPG approach to polymorphous and microcrystalline silicon semiconductors

R. I. BADRAN*, N. AL-AWWAD

Physics Department, The Hashemite University, P.O. Box 150459, Zarqa, Jordan

Further information on electronic properties, like trapped carrier density, for hydrogenated microcrystalline and polymorphous silicon thin films prepared by hot-wire chemical vapor deposition (HWCVD) and plasma-enhanced chemical vapor deposition (PECVD) techniques can be deduced from the experimental data of the high electric field dependence of the coefficient β in the steady-state photocarrier grating (SSPG) technique. This is achieved by adopting a convenient theoretical approach of the SSPG problem based on the small-signal photocurrent to fit the experimental data at different grating periods and temperatures. The values of small-signal mobility lifetime product, the drift (diffusion) lengths for holes and electrons can be estimated by exploiting the relations among the transport parameters. The correlation between the photoelectronic properties and the trapped carrier density is also discernable. The trapped carrier density values are also obtained from the adopted approach and compared to corresponding values using other approaches.

(Received February 16, 2006; in revised form May 2; accepted after revision June 28, 2006)

Keywords: Microcrystalline silicon, SSPG approach, Charge carrier

1. Introduction

An important feature in using SSPG technique over other techniques is observed in the convenient theoretical treatment of SSPG problem [1-6] which can provide us with information about the transport parameters of the investigated thin film semiconductors such as mobility lifetime product ($\mu\tau$) for charge carriers etc., in addition to the ambipolar diffusion length.

A significant advancement in understanding the transport and recombination of photocarriers of a semiconductor using SSPG experiment was achieved when this experiment was carried out at high electric fields. Here the measurement of the small-signal photocurrent depends on the grating period Λ which, in turn, varies as the angle of incidence of the two laser beams in SSPG experiment. The SSPG transport equations were solved via different approaches [3-6] on the basis of a small-signal grating of optical excitation superimposed on a much stronger uniform background generation of electron-hole pairs, by considering both lifetime and relaxation time regimes. The analytical treatment of steady-state transport equations in the small signal case based on the perturbation expansion theory was conducted, to the first order, in one approach [4] and thereafter extended to the second order, in another approach [5]. The latter approach has the advantage of avoiding previous assumptions of restriction on local charge neutrality and in considering the drift mobility and effective diffusion coefficient for electron and holes as concentration dependent. Therefore the correction of the SSPG theory in the relaxation-time regime was implemented and the importance of space charge effects was revealed in this

regime. A global expression for the coefficient β , which is known as the ratio of measured photocurrent density due to coherency of the two laser beams to an ac photocurrent density due to incoherency of these beams in SSPG experiment, was found and showed to contain two components relevant to drift and diffusion currents. An extended technique to measure accurately the diffusion length by removing the inherent defects in the original SSPG theory, was demonstrated by a successful application to hydrogenated amorphous silicon [5].

This paper concentrates on the investigation of the field and temperature dependence of the coefficient β and the transport parameters by developing a computer program to fit the experimental data for different polymorphous and microcrystalline silicon thin film samples, according to Hattori et al. approach [5]. The samples were prepared either by PECVD (initialized in the text with letter L, like L704232) or by HWCVD technique (initialized with letter R, like R808121, R260952, etc.). The dark conductivity values for the $\mu\text{C-Si:H}$ L704232 sample at 300, 129 are $8.76 \times 10^{-8} \text{ S.cm}^{-1}$, $2.0 \times 10^{-10} \text{ S.cm}^{-1}$, respectively and that at 115K is not measurable. Also the dark conductivities at room temperature for $\mu\text{C-Si:H}$ R808121, R2609052 samples are $15.8 \times 10^{-6} \text{ S.cm}^{-1}$, $4.72 \times 10^{-6} \text{ S.cm}^{-1}$, respectively and *pm-Si:H* L810081, L810083 samples are both not measurable, because they are lower than the limit of the measurement equipment [7]. The application of Hattori et al. approach on a set of experimental data may enable us to extract important information on the electronic properties (like small signal mobility-lifetime product of charge carriers and recombination lifetime) and to estimate the trapped carrier

density. The correlation among the transport parameters may also allow us to estimate other important physical quantities like the drift and diffusion lengths for electrons and holes. Finally, the normalized grating amplitudes formulas for electrons and holes are obtained using Hattori et al. approach and were employed in the final expression of the coefficient β as well. The diffusion lengths which were determined from fitting the experimental data in the low-field diffusion regime were employed to fit the experimental data for a wide range of electric fields [8]. We found that this assumption can be done within the illumination level (with a photon flux of $1.1 \times 10^{17} \text{cm}^{-2}\text{s}^{-1}$) of the conducted SSPG experiment for most of microcrystalline and polymorphous samples under investigation where it yields good results except one sample (with a photon flux of $6 \times 10^{16} \text{cm}^{-2}\text{s}^{-1}$) which gives less precise results. We have also used the expression for the density of states (DOS), from the exploitation of SSPG technique, which was derived for amorphous semiconductors [9,10] in order to roughly estimate DOS for polymorphous and microcrystalline semiconductors. The values of density of states from this expression are compared to those extracted from the adopted approach and other approaches.

2. A brief theoretical approach

In Hattori et al approach [5], the transport equations were solved with assumptions made to avoid the pitfalls of the original SSPG analysis [1-2,4]. The first assumption was to include the effect of the space-charge at high electric fields in addition to the case of local charge neutrality at low fields. Another assumption was made considering the drift mobility and effective diffusion constant as concentration dependent parameter. The SSPG theory was also extended by including second order term in perturbation expansion. A more accurate form of the coefficient β was derived [5]:

$$\beta = 1 - 2\gamma\gamma_0^2\Gamma \quad (1)$$

The parameter γ is the exponent in the power-law light intensity dependence of photoconductivity. We will consider here, the simplified version of the SSPG parameter Γ by neglecting some minor terms in the original expression [5], namely: $\Gamma = \frac{n_k p_k \sin(\Phi)}{KL_{diel}}$,

where $K = \frac{2\pi}{\Lambda}$, n_k and p_k are the normalized grating amplitudes of electron and hole concentrations. The grating amplitudes are expressed as [5]:

$$n_k = \frac{|\tilde{n}_k|}{g_k \tau'}, \quad (2)$$

and

$$p_k = \frac{|\tilde{p}_k|}{g_k \tau'}, \quad (3)$$

where \tilde{n}_k and \tilde{p}_k are complex numbers of the first-order carrier concentration of electrons, $\Delta N_1 = \tilde{n}_k \cos\left(\frac{2i\pi x}{\Lambda}\right)$,

and holes $\Delta P_1 = \tilde{p}_k \cos\left(\frac{2i\pi x}{\Lambda}\right)$, respectively. Each may

give the amplitude and phase of ΔN_1 , and ΔP_1 . Here,

$g_k \tau'$ is given by [5]:

$$g_k \tau' = \tilde{n}_k \left(\delta + \frac{ba}{(b+1)} - iKL_{en} + K^2 L_{dn}^2 \right) + \tilde{p}_k \left(\eta - \frac{ba}{(b+1)} \right), \quad (4.a)$$

or:

$$g_k \tau' = \tilde{n}_k \left(\delta - \frac{a}{(b+1)} \right) + \tilde{p}_k \left(\eta + \frac{a}{(b+1)} + iKL_{ep} + K^2 L_{dp}^2 \right), \quad (4.b)$$

where, $L_{en,p} = \mu'_{n,p} E_0 \tau'$, and $L_{dn,p} = (D'_{n,p} \tau')^{1/2}$ are

the drift and diffusion lengths for electrons and holes, respectively. The dimensionless transport parameters are

defined as $b \equiv \frac{\mu_n}{\mu_p}$, $a \equiv \frac{\tau'}{\tau_{diel}}$, $\delta = \frac{\tau'}{\tau'_n}$, and

$\eta = \frac{\tau'}{\tau'_p}$, where $\delta + \eta = 1$. The drift mobility for

electrons and holes are defined by

$$\mu_n(N) = \mu_n^f \frac{N^f}{N}, \quad (5)$$

and $\mu_p(P) = \mu_p^f \frac{P^f}{P}$. (6)

Also $\mu'_n(N) = \mu_n^f \left(\frac{dN^f}{dN} \right)_0$ and $\mu'_n(P) = \mu_p^f \left(\frac{dP^f}{dP} \right)_0$ are first order terms in the drift mobility defined in terms of the unperturbed parameters, where $()_0$ represents

unperturbed case. N^f (or P^f) represents the free electron (or hole) concentration and, N (or P), is the total electron (or hole) concentration which consists of trapped concentration N^t (or P^t), in addition to free concentration N^f (or P^f). These small-signal quantities also depend on the drift mobilities of free electrons and holes, μ_n^f and μ_p^f , respectively. The effective diffusion constants for electrons and holes are expressed by

$D'_n = D_n^f \left(\frac{dN^f}{dN} \right)_0$ and $D'_p = D_p^f \left(\frac{dP^f}{dP} \right)_0$ respectively,

where D_n^f and D_p^f are diffusion constants for free carriers. Another dimensionless constant $b' = (\mu'_n / \mu'_p = L_{en} / L_{ep} = L_{dn}^2 / L_{dp}^2)$ can be introduced as well. A common small-signal lifetime is defined

as $\tau' = \frac{\tau'_n \tau'_p}{\tau'_n + \tau'_p}$, where $\tau'_n = \left(\frac{dN}{dR} \right)_0$, $\tau'_p = \left(\frac{dP}{dR} \right)_0$,

and $\tau = \left(\frac{N}{R} \right)_0$. The recombination rate R is expressed

elsewhere [5] in the form of perturbation series. However, the dielectric relaxation time τ_{diel} is related to the background conductivity $\sigma_0 (= e(\mu_n + \mu_p)N_0)$ by

$\tau_{diel} = \frac{\epsilon_0 \epsilon_r}{\sigma_0}$. The dielectric relaxation length is also

defined by $L_{diel} = (\mu'_n + \mu'_p)E_0 \tau_{diel}$. The phase shift between electron and hole concentration gratings is $\Phi = Arg(\tilde{n}_k) - Arg(\tilde{p}_k)$.

3. Results

When equations 2 and 3 are simultaneously solved for \tilde{n}_k and \tilde{p}_k , the solutions are:

$$\tilde{p}_k = \frac{g_k \tau'}{\left(\eta - \frac{ba}{(b+1)} \right)} - \tilde{n}_k \frac{\left(\delta + \frac{ba}{(b+1)} - iKL_{en} + K^2 L_{dn}^2 \right)}{\left(\eta - \frac{ba}{(b+1)} \right)}. \quad (7)$$

and

$$\tilde{n}_k = \frac{g_k \left((a + K^2 L_{dp}^2) + iKL_{ep} \right)}{\left[\left(a + K^2 \left(\delta_{dp}^2 + L_{en} L_{ep} + L_{dn}^2 \left(\eta + \frac{a}{(b+1)} \right) + L_{dp}^2 \left(K^2 L_{dn}^2 + \frac{ba}{(b+1)} \right) + iK \left[\eta L_{en} - \delta_{dp} + \frac{a(L_{en} - bL_{ep})}{(b+1)} \right] \right) \right]}. \quad (8)$$

Further mathematical manipulations of equations 7 and 8 yield:

$$\tilde{n}_k = g_k \tau' \frac{(\kappa + i\zeta)}{\chi}. \quad (9)$$

where

$$\begin{aligned} \zeta &= K \left[\eta a (L_{en} + L_{eb}) + \frac{a^2 (L_{en} - bL_{eb})}{(b+1)} \right] + K^3 \left[(L_{dn}^2 L_{ep} + L_{en} L_{dp}^2) \left(\eta + \frac{a}{(b+1)} \right) + L_{en} L_{ep}^2 + L_{dn}^2 L_{dp}^2 K^2 L_{ep} \right] \\ \kappa &= a^2 + K^2 \left[L_{en} L_{ep} \left(a - \eta - \frac{a}{(b+1)} \right) + L_{ep} \left(\delta + \frac{ba}{(b+1)} \right) + cL_{dp}^2 \left(1 + \delta + \frac{ba}{(b+1)} \right) \right] \\ &+ aL_{dn}^2 \left(\eta + \frac{a}{(b+1)} \right) + K^4 \left[aL_{dn}^2 L_{dp}^2 \left(\frac{b+2}{b+1} \right) + L_{dp}^2 (L_{en} L_{ep} + \eta L_{dn}^2) + L_{dp}^4 (K^2 L_{dn}^2 + \delta + \frac{ba}{(b+1)}) \right], \end{aligned}$$

and

$$\begin{aligned} \chi &= \left\{ a + K^2 \left[L_{dn}^2 \left(\eta + \frac{a}{(b+1)} \right) + L_{dp}^2 \left(K^2 L_{dn}^2 + \frac{ba}{(b+1)} \right) + \delta L_{dp}^2 + L_{ep} L_{en} \right] \right\}^2 + \\ &\left\{ K \left[\eta L_{en} - \delta L_{ep} + \frac{a(L_{en} - bL_{ep})}{(b+1)} \right] \right\}^2. \end{aligned}$$

In the same way a simplified expression for the grating amplitude of holes \tilde{p}_k can be obtained:

$$\tilde{p}_k = g_k \tau' \left(\frac{(\chi - \kappa Z - \zeta \rho) + i(\kappa \rho - Z \zeta)}{\chi \xi} \right). \quad (10)$$

Here, $Z = \left(\delta + \frac{ba}{(b+1)} + K^2 L_{dn}^2 \right)$, $\xi = \left(\eta - \frac{ba}{(b+1)} \right)$

and $\rho = KL_{en}$.

Now, the normalized grating amplitudes n_k and p_k that were defined in equations 2 and 3, can be simply obtained by taking the modulus of equations (9) and (10), respectively, and then dividing each of them by $g_k \tau'$. Hence the normalized grating amplitude for electrons is:

$$n_k = \sqrt{\frac{k^2 + \zeta^2}{\chi^2}} \quad (11)$$

and the corresponding amplitude for holes is:

$$p_k = \sqrt{\frac{(\chi - \kappa Z - \zeta \rho)^2}{\chi^2 \xi^2} + \frac{(\kappa \rho - Z \zeta)^2}{\chi^2 \xi^2}}. \quad (12)$$

Also the phase shift between the two grating amplitudes is found to be:

$$\Phi = \tan^{-1} \left(\frac{\zeta}{k} \right) - \tan^{-1} \left(\frac{\kappa \rho - Z \zeta}{\chi - \kappa Z - \zeta \rho} \right). \quad (13)$$

Four transport parameters seems to play the major role in Hattori *et al* approach [5], namely, $b (= \mu_n / \mu_p)$, $b' (= \mu'_n / \mu'_p)$, $a (= \tau' / \tau_{diel})$ and $\varphi' (= \gamma \gamma_0^2)$. A computer code is developed and used to test this adopted approach on a set of experimental data for different polymorphous and microcrystalline semiconductor silicon samples. The values of ambipolar diffusion length L_{amb} and γ obtained from the low field fit for different silicon samples [8] in addition to quality factor of $\gamma_0 = 1$ are used as input data in the simulations. Reasonable fits are obtained to all experimental data using five adjustable parameters, namely, μ_n , μ_p , μ'_n , μ'_p and a . The search for the accurate values of these parameters is based on minimizing the errors between the experimental data and calculations. The fits to the experimental data of the coefficient β versus applied electric field at different grating periods Λ , when the SSPG experiment is conducted at 300, 129 and 115K for the $\mu\text{C-Si:H}$ sample L704232 are presented in Fig. 1. The parameter γ , which is the exponent (usually takes a value between 0.5 and 1) of the power-law dependency of the photoconductivity versus the generation rate, is given the

values 0.68, 0.65 and 0.62 for this sample at 300, 129 and 115 K, respectively. Also the fittings to experimental data of μC -Si:H samples R808121 and R2609051 and of pm -Si:H samples L810081 and L810083 at 300 K are shown in Figs. 2 and 3, respectively. In all these figures, the error bars indicate the deviations of our calculated values from the experimental data within an average value 10% for all experimental errors. All adjustable parameters are summarized in Table 1. Here the values of γ are 0.62, 0.5, 0.62 and 0.7 for the samples R808121, R2609051, L810081 and L810083 respectively. However, the values of parameters $b(= \mu_n/\mu_p)$ and $b'(= \mu'_n/\mu'_p)$ are not listed here. The parameter, $b=7.89$ for μC -Si:H sample L704232 at 300K, as an example, is found invariant, while the value of b' changes from 1.63 to 4.2 when the grating period changes from 2702 nm to 905 nm. When the temperature is lowered to 129K, lesser values of $b=3.26$ and $b'=0.52$ are needed to fit the data. A further decrease in temperature to 115 K may lead to corresponding values of $b=2.65$ and $b'=0.31$. The small-signal parameters μ'_n , τ' and the hole mobility μ_p are found more sensitive than μ'_p and μ_n parameters in fitting the experimental data as the temperature decreases in all of the samples. Also the parameters μ'_n , μ'_p and τ' are found sensitive to the change in grating period. Here the fall off in the values of μ_n when the temperature is lowered from 300 K down to 115 K for this microcrystalline sample of thickness $0.34 \mu\text{m}$ is from $(0.0015\text{-}0.00135) \text{ cm}^2\text{V}^{-1}\text{s}^{-1}$. In general, such fall-off is shallower than the fall off for a thicker pm -Si:H samples (of 3.3 and $5.9 \mu\text{m}$) studied by time-of-flight experiment [11]. However the hole drift mobility exhibits opposite behavior with the decrease in temperature. A comparison with the experimental hole mobility results could not be made because the TOF drift mobility depends essentially on the free carrier mobility and on the shallow band tail states. In addition, this TOF experiment [11] does not cover the same range of temperatures considered in our SSPG experiment. Moreover the calculated values of hole mobility at low temperatures are in the same order of magnitude as those recently measured elsewhere [12] using transient photocurrent technique. Also, our hole mobility values at room temperature disagree by two orders of magnitude with those measured by the previous technique and three order of magnitude by those found by the field-effect hole mobility measurement [13]. It must be noted here that our analysis asserts the temperature dependency of electron or hole motilities in microcrystalline and polymorphous silicon underlined by others [11,12].

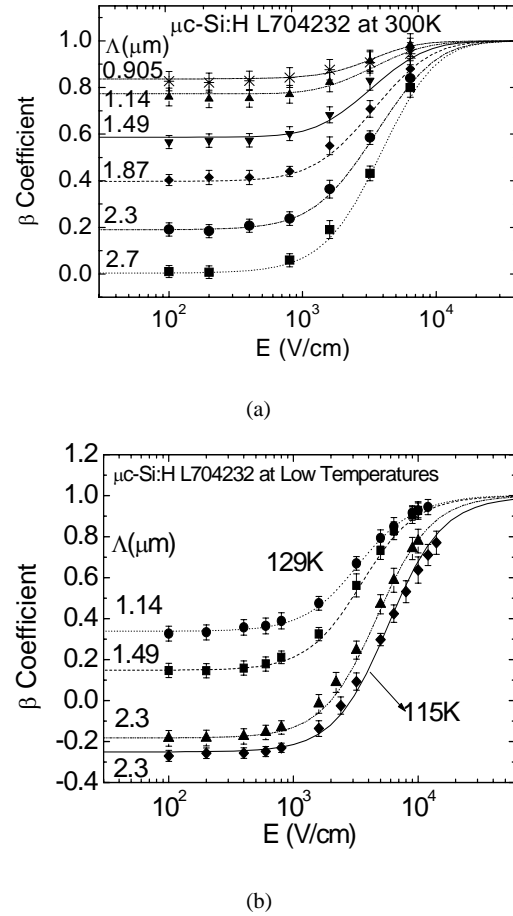


Fig. 1. The field dependence experimental data (symbols) of the coefficient β for μC -Si:H sample L704232 at different grating periods and at different temperatures. The theoretical results (lines) are obtained using equation 1 with the free parameters listed in Table 1.

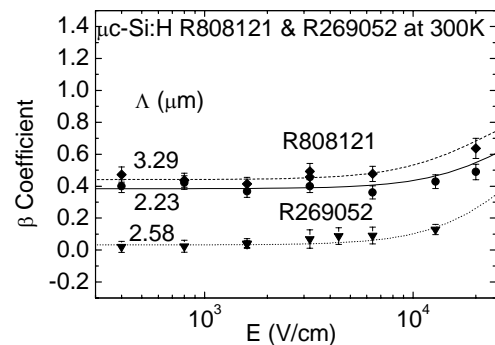


Fig. 2. Same as in Fig. 1, but for μC -Si:H R808121 and R269052 samples at different grating periods and at room temperature.

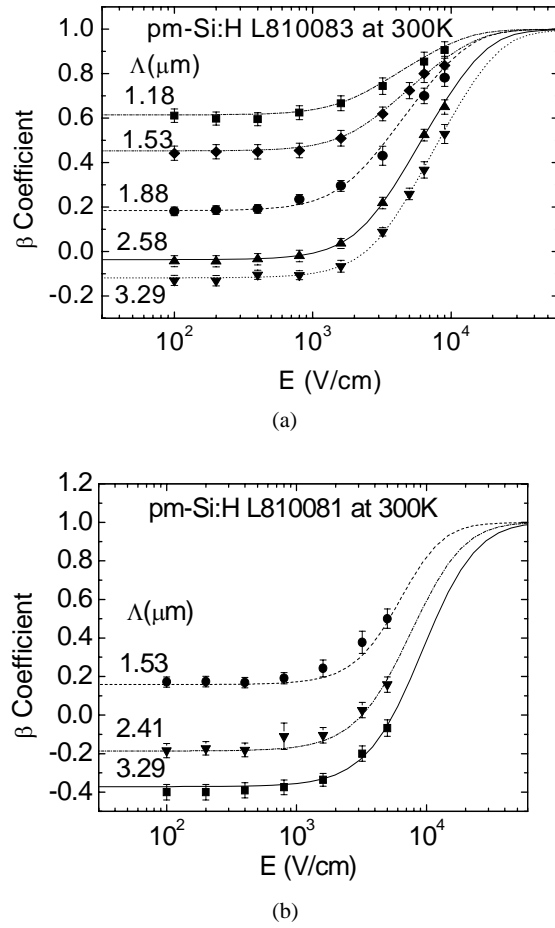


Fig. 3. Same as in Fig. 1 but for *pm*-Si:H L810083 and L810081 samples at different grating periods and at room temperature.

A reasonable fit could not be reached unless δ is close to unity and $\eta = 0$ at the generation rate of $G_0 = 1.633 \times 10^{20} \text{ cm}^{-3} \text{ s}^{-1}$ for μC -Si:H sample L704232 at 300 K, as an example. This assumption means that a larger value of hole lifetime τ'_p than that of the electron lifetime τ'_n is discernible. Therefore $\delta = 1$ and $\eta = 0$ are considered in all fittings where the generation rate has the same order of magnitude in all samples under study.

A crude approximation can be made in determining the diffusion lengths $L_{dn,p}$ for electrons and holes using a simplified expression for the ambipolar diffusion length $L_{amb} = \left[(\mu_n L_{dp}^2 + \mu_p L_{dn}^2) / (\mu_n + \mu_p) \right]^{1/2}$ [5]. Here the value of ambipolar diffusion length obtained from the fit to experimental data at the low field can be used together with the transport parameters b and b' (obtained from Table 1) extracted from the electric field dependence of

β , to estimate the values of $L_{dn,p}$. We do that, because there are no large differences between the values of the transport parameters a and b (apart from the sample *pm*-Si:H L810083) where the value of L_{amp} is not seriously deviated from that of L_{app} proposed in Ref 5. Also the values of $L_{en,p}$ can be estimated using the relation $L_{en,p} = \mu'_{n,p} E_0 \tau'$. The values of $L_{dn,p}$ and $L_{en,p}$ for μC -Si:H sample L704232 at 300, 129 and 115K using L_{amb} of 226, 135 and 118 nm, respectively, obtained from the fits are all listed in Table 2. All these calculations are carried out using $E_0 \approx E_d = \frac{2\pi k_B T}{e\Lambda}$ with $\Lambda = 2300 \text{ nm}$ and τ' equal 0.266×10^{-6} , 2.38×10^{-6} and $5.12 \times 10^{-6} \text{ s}$ at the temperatures 300, 129 and 115K, respectively. Also the average drift length of electrons and holes can be estimated to be approximately $0.226 \mu\text{m}$ for the or μC -Si:H sample L704232 at 300K when the values of $L_{en} = 0.281 \mu\text{m}$ and $L_{ep} = 0.172 \mu\text{m}$ in Table 2 are considered. This can be compared to a corresponding approximate average value of $0.22 \mu\text{m}$ found from the formula $\langle L_{drift} \rangle = (\mu_n \mu_p)^{1/2} \tau E_0$ [4], for the same sample when E_0 is taken approximately equal to $E_d (= 706.2 \text{ V/cm})$ at $\Lambda = 2300 \text{ nm}$ and the small signal parameters replace μ_n, μ_p and τ .

The normalized grating amplitude for electrons and holes, n_K and p_K , and their phase shift Φ , in equations (11-13), are plotted versus the applied electric field and the parameter a . The plots are shown in Fig. 4. It is also worth noting that the analysis may be conducted under the condition of a regime in which the carrier lifetime is a bit larger than the dielectric relaxation time. This condition is justified here because the value of adjustable parameter $a = (\tau'/\tau_{diel})$ is larger than unity for most of the samples under study. The μC -Si:H sample L704232 at 300K with $b = 7.89$, $a = 2.0$, $\delta = 1$ and $\Lambda = 2702 \text{ nm}$ (i.e. $\Lambda \approx 12 L_{amb}$) is taken here as an example. Fig. 4-a shows the expected features in the reduction of the normalized amplitudes when the applied electric field increases. Fig. 4-b also shows that such increase in electric field also leads to a change in the phase shift between the amplitudes of electrons and holes from zero at low electric field to almost 180° at high fields. This is consistent with the global behavior of both charge carriers when the local charge neutrality is satisfied and the effective diffusion length is L_{amb} [3] at low electric fields. It is also in agreement with the behavior of space charge effects when the two kinds of charge carriers are moving

independently under the effect of high electric field and L_{amb} does not represent anymore the actual effective diffusion length [5]. Also, at a fixed electric field, the variation of a from low values to high values, shown in Fig. 4-c, represents a transition from diffusion-dominated to drift-dominated process. This behaviour is found similar to that appeared in Ref 3. This also makes the phase shift between the amplitudes of electrons and holes to change from large values to almost zero as a changes from low to high values, as in Fig. 4-d. The value of $b = 7.89$, here, is not so large compared to the value of $a = 2.0$ so that the use of values of L_{amp} in our simulations can be justified as these values do not largely deviate from L_{app} proposed in Ref [5]. We admit that there is a serious discrepancy for the case of the sample pm -Si:H L810083

which has $b = 39.2$ compared to $a = 4.5$. However, the value of $a = 2.0$ has a corresponding value of $\tau' = 0.266 \times 10^{-6} s$ for μc -Si:H sample L704232 at the temperatures 300 K. Using this value of τ' may further lead to an estimation to mobility-lifetime product, *i.e.* $(\mu'_n + \mu'_p)\tau' = 0.64 \times 10^{-9} cm^2 V^{-1} s^{-1}$ when the values of $\mu'_n = 1.5 \times 10^{-3} cm^2 V^{-1} s^{-1}$ and $\mu'_p = 0.92 \times 10^{-3} cm^2 V^{-1} s^{-1}$, listed in Table 1, for this sample at temperature 300 K are utilized.

Table 1. The list of parameters used to fit the experimental data of electric field dependence of β for different polymorphous and microcrystalline silicon samples at different grating periods and different temperatures, using equation 1. Here $\delta = 1$, and $\eta=0$ are chosen.

Sample	$\Lambda(nm)$	$a = \frac{\tau'}{\tau_{diel}}$	$\mu_n \times 10^{-2}$ ($cm^2 V^{-1} s^{-1}$)	$\mu_p \times 10^{-2}$ ($cm^2 V^{-1} s^{-1}$)	$\mu'_n \times 10^{-3}$ ($cm^2 V^{-1} s^{-1}$)	$\mu'_p \times 10^{-3}$ ($cm^2 V^{-1} s^{-1}$)
μc -Si:H L704232 at 300 K	2702	2.0	1.5	0.19	1.5	0.920
	2300	2.0	1.5	0.19	2.7	0.944
	1837	2.15	1.5	0.19	2.9	0.935
	1490	2.2	1.5	0.19	3.2	0.949
	1140	2.45	1.5	0.19	3.3	0.951
	905	2.6	1.5	0.19	4.0	0.952
μc -Si:H L704232 at 129 K	2300	5.5	1.4	0.43	0.5	0.961
	1490	5.9	1.4	0.43	0.8	0.964
	1140	6.2	1.4	0.43	0.9	0.967
μc -Si:H L704232 at 115 K	2300	9.9	1.35	0.51	0.3	0.967
μc -Si:H R808121at 300 K	3290	0.5	1.30	0.57	1.9	1.496
	2230	0.77	1.30	0.57	2.3	1.2637
	1180	0.92	1.30	0.57	2.4	1.263
μc -Si:H R2609052 at 300 K	2580	0.7	1.30	0.57	2.0	1.266
pm -Si:H L810081at 300 K	3290	2.3	1.00	0.10	0.5	0.238
	2410	2.5	1.00	0.10	1.2	0.517
	1530	2.8	1.00	0.10	2.5	0.936
pm -Si:H L810083 at 300 K	3290	4.4	4.7	0.12	2.4	4.363
	2580	4.4	4.7	0.12	2.5	4.464
	1880	4.5	4.7	0.12	2.7	4.576
	1530	4.6	4.7	0.12	2.8	4.666
	1180	4.8	4.7	0.12	2.8	4.179

Table 2. The ambipolar, electron, and hole diffusion and drift lengths for microcrystalline silicon sample L704232 at different temperatures.

T(K)	L_{amb} (nm)	L_{dn} (nm)	L_{dp} (nm)	L_{en} (nm)	L_{ep} (nm)
300	226	278.83	218.4	281.77	172.82
129	135	103.30	143.30	361.28	694.38
115	118	71.10	127.70	415.81	1340.3

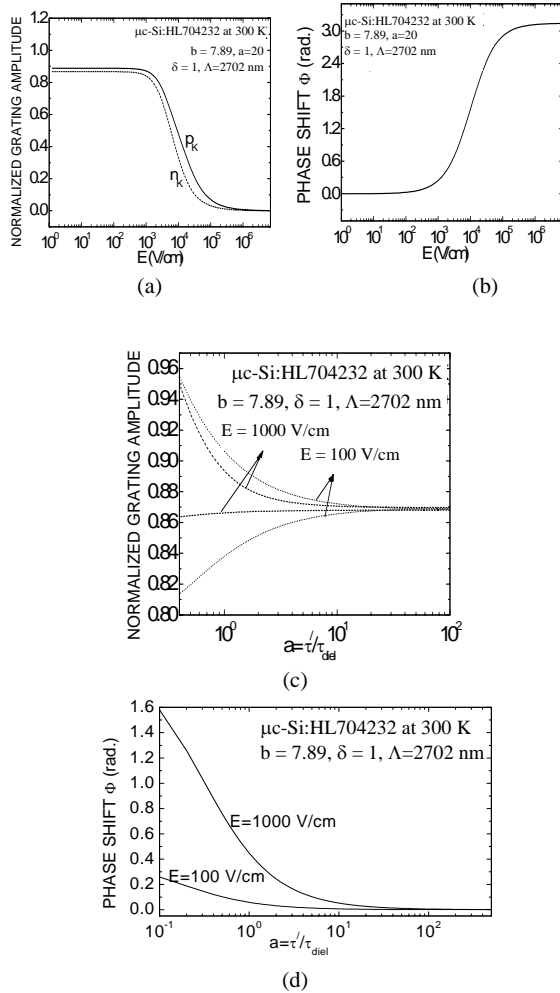


Fig. 4. (a) The normalized grating amplitudes n_K and p_K in equations (11) and (12) are plotted versus applied electric field. (b) The phase angle Φ between amplitudes in equation (13) is plotted versus electric field at $a = 2$. (c) The normalized grating amplitudes n_K and p_K are plotted against a at two values of electric field. (d) The phase angle Φ is plotted versus a at two values of electric field. All graphs are for $\mu\text{C-Si:H}$ sample L704232 at 300 K.

Further exploitation to the field dependence SSPG approach can be achieved by calculating the trapped carrier density N_t . This calculation can be conducted if the assumptions made by other groups [4, 5] are considered such that the photocarrier density $N_{pc} \approx \frac{\tau'G_o}{\gamma}$. Also further assumption is made,

here, such that N_0 is very much greater than the free-carrier density (i.e. $N_o \approx N_t \approx N_{pc}$). Similar assumptions are adopted to estimate N_t , by using Li approach [4]. However N_0 is obtained, due to Abel et al. approach [6], from the fitting parameter $\mu_n \tau_{rel}^{eff} \approx (\epsilon_r \epsilon_o / e N_o)$ by considering that $N_0 \approx N_t$ [8]. The carrier density N_t has also been determined using Schmidt-Longeaud formula [9, 10]. It is assumed that photoconductivity σ_{ph} replaces the factor σ_0 available in their formula of DOS for each sample under study. The values of μ_n obtained from the fits (in Table 1) together with the values of the generation rate G_o , γ and σ_{ph} obtained from experiment are used. The ratio $\frac{G_2}{G_1}$ is

given a value of 0.06 for most of the samples and $C_n = 10^{-8} \text{ cm}^3 \text{ s}^{-1}$. All results of N_0 are listed in Table 3.

There is excellent agreement among the values of N_0 for all samples due to Li and Hattori et al. approaches where the same formula is adopted. However the values obtained from Abel et al fit are approximately equal to those obtained from Li and Hattori et al. approaches for all cases except those of the samples L704232, R808121 and R2609052 at 300 K. Although the values of N_0 obtained from Schmidt-Longeaud formula are different from all other corresponding values, but the increase in the density of states as the temperature decreases is prominent. Also the different values of N_0 is consistent with the corresponding values of $(\mu\tau)_p$ product in most of the samples. It is worth noting that the estimation of N_0 in all these approaches is not accurate due to the several approximations involved in each approach. However these values of N_0 are within the same order of magnitude to that obtained from capacitance measurements for pm-Si:H samples and differ with other values reported in the literature [14]. These calculations, however, give us a glimpse of the behavior of the trapped carrier density as deduced from SSPG technique when the temperature or the $(\mu\tau)_p$ product differs.

Table 3. The density of state values for different μc -Si:H and pm -Si:H samples at different temperatures obtained from application of Abel et al., Li, Hattori et al. and Schmidt-Longeaud approaches are compared.

Si:H Sample	$\Lambda(\text{nm})$	$N_0 \times 10^{14}$ (cm^{-3}) (Li)	$N_0 \times 10^{14}$ (cm^{-3}) (Hattori)	$N_0 \times 10^{14}$ (cm^{-3}) (Abel)	$N_0 \times 10^{14}$ (cm^{-3}) (Schmidt)
μc - L704232 at 300 K	2702	0.64	0.64	5.0	0.020
μc - L704232 at 129 K	2300	6.0	5.98	6.7	0.078
μc - L704232 at 115 K	2300	13.5	13.48	10.3	0.083
μc - R808121 at 300 K	3290	0.23	0.22	25.1	0.035
μc - R2609052 at 300 K	2580	0.41	0.41	50.2	0.067
pm - L810081 at 300 K	3290	11.4	11.38	12.1	0.267
pm - L810083 at 300 K	3290	14.9	14.88	15.4	0.665

4. Discussion

There is a reasonable consistency in the variation of N_0 values obtained from four approaches for most of the samples. In particular, it is evident that the decrease in temperature results in decreasing the field-dependent β and increasing the trapped charge density for the μc -Si:H L704232 at 300K. This can be taken together with the values of $(\mu\tau)_p$ product, found from the low field fit, as an indication of a steep valence-band tail distribution, which, if it was wide, would result in a much higher trapped charge density. It is also evident that there is a

pronounced correlation between the trapped charge density and the minority carrier mobility-lifetime product for different samples. However, it is obvious that the two chosen samples μc -Si:H R808121 and R2609052 with low $(\mu\tau)_p$ product do not show much larger values of N_0 than the samples with high $(\mu\tau)_p$ due to all approaches except that of Abel et al. approach. This is attributed to incorrect application of the assumed formula of $N_{pc} \approx \frac{\tau'G_0}{\gamma}$ to these samples as the dark current is higher (1230 nA in R808121 sample) or comparable (230.3 nA in R2609052 sample) to the corresponding photocurrents 510 nA and 249.7 nA, respectively. This is also attributed to our assumption of replacing σ_0 by photoconductivity in Schmidt-Longeaud formula. It can be noted that the obtained values of N_0 for these samples, from Abel et al. approach, are more precise because the latter assumptions are not considered here. However, it must be emphasized that this correlation between transport

properties and sub-gap absorption is not a general rule but is also dependent on the Fermi-level position and to some degree on optical scattering [15]. Therefore, we claim that the increase in sub-gap absorption is consistent with the larger trapped charge density revealed in the field-dependent SSPG experiments in most of the cases.

The sensitivity of the transport parameters b and b' to the change in temperature asserts that drift mobility and effective diffusion constant must be concentration dependent. This means that this model could deal properly with the trap-controlled photocarrier transport, which would occur in the polymorphous and microcrystalline semiconductors with localized states distributed within the band gap. Accurate values of trapped carrier density can be obtained if a better formula for the trapped carrier density is used. In a manner similar to that in a standard a-Si:H, the effects of traps in these semiconductors in introducing the small signal transport parameters is very tangible, and the dependence of drift mobility and diffusion constant on trapped charge density in pm - and μc -Si:H samples can not be tolerated.

The nonzero parameters, $\frac{1}{\tau_n''}$ and μ_p'' , that do not appear in our simplified version of the expression of β [5], can be written as $\frac{\tau'}{\tau_n''} = \frac{1-\gamma}{2\gamma}$ and $\frac{\mu_p''}{\mu_n'} = \frac{T_V - T}{2\pi b'}$. Using the obtained results of b , b' and inserting $T = 300K$ and $T_V = 600K$ for the μc -Si:H sample L704232 in the above expressions, the values of 0.26 and 0.044 for $\frac{\tau'}{\tau_n''}$ and $\frac{\mu_p''}{\mu_n'}$ are

estimated, respectively. These values validate the use of our simplified expression of β in equation 1.

5. Conclusions

The electric-field dependence in the SSPG technique has been applied to hydrogenated polymorphous and microcrystalline semiconductor thin films prepared by plasma-enhanced chemical vapor deposition and hot-wire chemical vapor deposition techniques at different temperatures. The experimental data obtained from this technique that cover a wide range of applied electric field values, probe the whole transition region between the diffusion- and the drift-dominated transport. The analysis of these experimental data, via Hattori et al approach, leads to the extraction of more information on carriers transport in addition to the ambipolar diffusion length. It is found that the quality of agreement between theory and experiment is very sensitive to the choice of parameters. Slight changes in the small-signal adjustable parameters produce significant changes in the calculated coefficient β . Furthermore, the effect of each parameter on the coefficient β is found to be physically transparent and consistent with the prescription of the adopted approach. The correlation among some of the transport parameters used in fitting the experimental data enabled us to estimate the drift and diffusion lengths for holes and electrons in addition to small-signal mobility lifetime product. The exploitation of the electric-field dependence in this approach is correlating the photoelectronic properties, which are demonstrated by the transport parameters, to the trapped charge density which is usually not easily accessible. This may also justify the enhanced relationship between the minority carrier mobility-lifetime product and trapped charge density and then the sub-gap absorption in most of the samples under study. This theoretical investigation asserts using carrier mobility as concentration dependent parameters. It also demonstrates the weakness in the assumption of local charge neutrality and ambipolarity restriction. Our studies have clearly shown that the analysis of experimental data of electric field dependence, due Hattori et. al. approach, is more recommended than that of Li approach. Moreover, the agreement between the calculations and experimental data is considered reasonable in view of the approximations involved in using the adopted approach.

Acknowledgments

Both authors (R. I. Badran and N. AL-Awwad) are grateful to the Higher council of Science and Technology (HCST), Jordan and the Deutsche Forschungsgemeinschaft (DFG), Bonn, Germany for their support. The authors would like to thank Dr. Rudi Brueggemann, University of Oldenburg, for providing the experimental data and to H. Brummack and K. Bruhne from Institute fur Physikalische Elektronik, Universitat Stuttgart, for providing the samples.

References

- [1] D. Ritter, E. Zeldov, K. Weiser, Appl. Phys. Lett. **49** 791 (1986).
- [2] D. Ritter, K. Weiser, E. Zeldov, J. of App. Phys. **62**, 4563 (1987).
- [3] D. Ritter, K. Weiser, E. Zeldov, Phys. Rev. B **38**, 8296 (1988).
- [4] Y. M. Li, Phys. Rev. B **42**, 9025 (1990).
- [5] K. Hattori, H. Okamoto, Y. Hamakawa, Phys. Rev. B **45**, 1126 (1992).
- [6] C. D. Able, G. H. Bauer, W. H. Bloss, Phil. J Mag. B **72**, 51 (1995).
- [7] R. I. Badran, R. Brueggemann, Proc. of the 19th European Photovoltaic Solar Energy Conf. 3DV 1.28, Paris, France, p.1505 (2004).
- [8] R. Brueggemann, R. I. Badran, Mat. Res. Soc. Symp. Vol. **808**, A9.7.1 (2004).
- [9] J. A. Schmidt, C. Longeaud, Appl. Phys. Lett. **85**, 4412 (2004).
- [10] J. A. Schmidt, C. Longeaud, Phys. Rev. B **71**, 125208 (2005).
- [11] J. P. Kleider, M. Gauthier, C. Longeaud, D. Roy, O. Saadane, R. Brueggemann, Thin Solid films 403-404, 188 (2002).
- [12] T. Dylla, F. Finger, E. A. Schiff, Appl. Phys. Lett. **87**, 0321103 (2005).
- [13] L. C. Cheng, S. Wagner, Appl. Phys. Lett. **80**, 440 (2002).
- [14] S. Reynolds, V. Smirnov, F. Finger, C. Main, R. Carius, J. Optoelectron. Adv. Mater. **7**, 91 (2005).
- [15] R. Brueggemann, J. P. Kleider, C. Longeaud, Proc. of the 16th European Photovoltaic Solar Energy Conf. VB 1.62, Glasgow, UK, p.1/4 (2000).

*Corresponding author: rbadran@hu.edu.jo